

End-to-End Predictive Planner for Autonomous Driving with Consistency Models

Anjian Li^{†*}, Sangjae Bae[†], David Isele[†], Ryne Beeson^{*} and Faizan M. Tariq[†]

^{*}Princeton University, Princeton, NJ, USA

[†]Honda Research Institute, San Jose, CA, USA

Abstract—Trajectory prediction and planning are fundamental components for autonomous vehicles to navigate safely and efficiently in dynamic environments. Traditionally, these components have often been treated as separate modules, limiting the ability to perform interactive planning and leading to computational inefficiency in multi-agent scenarios. In this paper, we present a novel unified and data-driven framework that integrates prediction and planning with a single consistency model. Trained on real-world human driving datasets, our consistency model generates samples from high-dimensional, multimodal joint trajectory distributions of the ego and multiple surrounding agents, enabling end-to-end predictive planning. It effectively produces interactive behaviors, such as proactive nudging and yielding to ensure both safe and efficient interactions with other road users. To incorporate additional planning constraints on the ego vehicle, we propose an alternating direction method for multi-objective guidance in online guided sampling. Compared to diffusion models, our consistency model achieves better performance with fewer sampling steps, making it more suitable for real-time deployment. Experimental results on Waymo Open Motion Dataset (WOMD) demonstrate our method’s superiority in trajectory quality, constraint satisfaction, and interactive behavior compared to various existing approaches.

I. INTRODUCTION

To navigate safely and efficiently in a dynamic environment, autonomous vehicles must effectively predict and interact with diverse road participants, including other vehicles, pedestrians, and cyclists. This typically requires a prediction module to anticipate other agents’ future trajectories and a planning module to generate trajectories for the ego vehicle. While prediction modules have widely adopted data-driven approaches to learn from human-driving data, planning modules typically rely on optimization-based methods. These two modules usually operate in a decoupled, alternating manner [31, 10].

This decoupled method introduces fundamental limitations. The interactive behavior generated by the planner is inherently reactive rather than proactive, as the planner responds to other agents without accounting for how they might react to the ego vehicle. This limitation can lead to the computationally expensive theory of mind (TOM) reasoning [53, 12, 17, 18]. In highly interactive scenarios, such as lane merging where proactive nudging is essential, reactive planning may cause the ego vehicle to be stuck [3, 5]. Existing solutions either struggle to scale with the number of agents [25] or compromise optimality due to a restrictive exploration of the solution search space [49].

In addition, modular approaches optimize prediction and planning independently, which often leads to less effective

behavior compared to jointly trained, end-to-end frameworks [30]. The alternation between prediction and planning modules also introduces latency and computational inefficiency, making it challenging to meet the demands of real-time operation.

Our key insight is that modeling the joint distribution of future trajectories for both the ego vehicle and surrounding agents can unify prediction and planning into a single, end-to-end framework. In this approach, the ego trajectory, informed by the desired goal location, represents the plan, while the trajectories of surrounding agents serve as predictions. Additional planning constraints can be imposed on the ego trajectory as needed. When trained on large-scale human driving datasets like the Waymo Open Motion Dataset (WOMD) [15], this joint distribution naturally captures the complex interactive behaviors observed in real-world scenarios.

Diffusion models [51, 20] offer a promising method to sample from this high-dimensional, multimodal joint distribution of ego and surrounding agents’ trajectories. They have demonstrated success in generating high-quality images and videos [39, 21] or robot trajectories [38, 27]. Moreover, their ability to model conditional distributions makes them well-suited for trajectory planning applications, as it allows for the incorporation of crucial context for planning and prediction, including trajectory history, map information, ego vehicle’s goal locations, etc. Compared to transformers, diffusion-based method also supports controllable generation to accommodate additional requirements solely at test time through guided sampling, without any additional training.

However, diffusion models typically require many sampling steps to obtain high-quality samples, making it challenging to meet the demands of real-time operations on autonomous vehicles. To overcome this limitation, consistency models [52] are designed to generate data directly from noise in a single step or a small number of steps, significantly improving sampling efficiency without compromising quality.

In this paper, we present an end-to-end predictive planner based on consistency models, designed to unify planning and prediction within a single data-driven framework. Our method samples from the conditional joint distribution of ego and surrounding agents’ future trajectories, given encoded map and trajectory history along with the ego vehicle’s goal configuration. While we use a transformer-based scene encoder [45] in our implementation, our approach is encoder-agnostic and can integrate with any suitable scene encoder. Trained on WOMD [15], our method ensures proactive trajectory planning

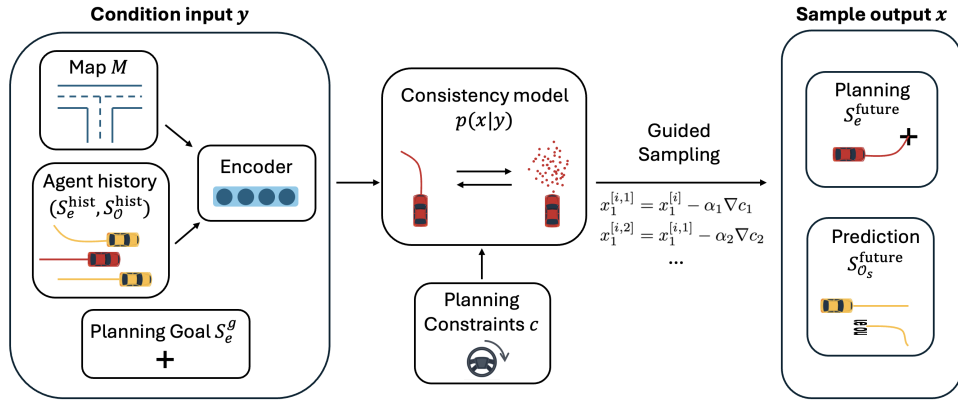


Fig. 1: The overview of our method.

by capturing complex interactions between agents observed in the real world. Additionally, during online testing, planning constraints are incorporated through guided sampling using our proposed alternating direction method for multi-objective guidance.

Experiments demonstrate that our consistency model-based planner generates effective interactive behaviors with other agents, such as nudging and yielding, through a single inference, eliminating the need for iterative alternation between prediction and planning modules. It outperforms diffusion models by requiring fewer sampling steps while delivering superior trajectory quality. Compared to transformer-based models, it enables controllable generation through online guided sampling that significantly improves planning constraint satisfaction.

II. RELATED WORK

For trajectory predictions, data-driven methods have shown promising results when trained on large-scale real-world human driving datasets such as Waymo Open Motion Dataset (WOMD) [15], INTERACTION Dataset [62], Argoverse [8] or nuScenes [7]. Graph Neural Networks have been used to model the semantic information in traffic scenarios for interactive prediction [23]. Generative models like Variational Autoencoders and Diffusion Models have also been utilized for multimodal trajectory prediction tasks [43, 27]. Recently, transformers [56], particularly Motion Transformers (MTR) [45, 46, 34] with encoder-decoder architectures, have achieved state-of-the-art results in trajectory prediction [58].

In trajectory planning, the goal is to determine a feasible and efficient path for the ego vehicle, based on observations of the environment and surrounding agents. This task is often formulated as a numerical optimization problem, typically decomposed path planning and speed planning to facilitate real-time operation in dynamic environments [60, 61, 2]. Game-theoretic approaches have been explored to model agent interactions [41], with efficient computation [16] that considers imperfect traffic agents [54], safe actions [55], and uncertainty reduction in the estimates of agent behaviors [22].

Beyond standalone planning, preliminary effort has been

made to integrate trajectory predictions into planner design for collision avoidance [31] and proactive motion planning [4, 44, 49]. While the aforementioned methods have advanced trajectory prediction and planning performance in dense environments, to our best knowledge, none have attempted to unify these two to achieve *human-like* interactive behavior with computational efficiency. Instead, our work addresses this gap by presenting a data-driven framework for end-to-end joint prediction and planning with a single inference.

Diffusion models [47, 51, 20] are generative models capable of producing high-quality samples from complex distributions, initially achieving success in image and video generations [39, 21]. The Denoising Diffusion Probabilistic Model (DDPM) [20] gradually corrupts the training data with Gaussian noise and learns to reverse this process through iterative denoising with deep neural networks. These models commonly use U-Net [40] or transformer-based architectures [56] as backbones. Conditional sampling in diffusion models is enabled by techniques such as classifier guidance [13] and classifier-free guidance [19]. However, DDPM requires numerous sampling steps to preserve the sample quality, resulting in significant computational costs. To address this inefficiency, Denoising Diffusion Implicit Models (DDIM) [48] introduces a deterministic generation process that balances sampling quality and speed, while progressive distillation [42] reduces the number of sampling steps by distilling a pre-trained diffusion model into a more efficient one. Consistency model [52, 50] takes a different approach, directly generating data from noise. They can be trained through distillation of a pre-trained diffusion model or a standalone consistency training and outperform distillation methods in one- and few-step sampling [52].

Diffusion and consistency models also have shown success in robotics and autonomous systems for their expressiveness and ability to provide samples from complex distributions. In robotics, conditional diffusion models have been applied to policy learning [26, 1, 11], with consistency models following similar applications [14, 37]. Diffusion models have also been adopted for trajectory optimization across various robotics tasks [33, 32]. In autonomous driving, diffusion models have shown promising results in trajectory prediction [27, 57]

and controllable traffic simulation or scenario generation [63, 59, 9, 24], capturing complex interactive behaviors in traffic scenarios. However, our work differs fundamentally from these efforts: we focus on developing a predictive trajectory planner with consistency models, leveraging guided sampling to incorporate planning constraints. Unlike scenario generation tasks, where sampling efficiency is less critical, our consistency model-based predictive planner needs significantly shorter sampling steps to deliver high-quality interactive behaviors compared to diffusion models.

III. PROBLEM FORMULATION

We aim to plan the trajectory of the ego vehicle with a planning goal, simultaneously predicting the interactive behaviors of others. We assume the trajectory histories of traffic agents and map information are given and known.

At the current timestep $t_0 \in \mathbb{R}$, the ego agent's state history over the past $H_1 \in \mathbb{N}$ timesteps including the current state is given as $S_e^{\text{hist}} = (s_e^{t_0}, s_e^{t_0-1}, \dots, s_e^{t_0-H_1}) \in \mathbb{R}^{(H_1+1) \times d_s}$, where d_s is the dimension of the states, e.g. position, velocity, etc. Let \mathcal{O} denote the set of other agents of all types such as vehicles, pedestrians, and cyclists. Their history states are given for the current timestep t_0 and the past H_1 timesteps, denoted by $S_{\mathcal{O}}^{\text{hist}} = (s_o^{t_0}, s_o^{t_0-1}, \dots, s_o^{t_0-H_1})_{o \in \mathcal{O}} \in \mathbb{R}^{N_{\mathcal{O}} \times (H_1+1) \times d_s}$, where $N_{\mathcal{O}} = |\mathcal{O}|$. The map information is denoted by $M \in \mathbb{R}^{N_m \times c \times d_m}$, which includes $N_m \in \mathbb{N}$ polylines in the scenario with c points on each polyline and d_m attributes per point. We use fixed dimensions $N_{\mathcal{O}}$ and N_m for agents and map polylines respectively, which are chosen large enough to accommodate all scenarios with padding and masks applied to invalid entries. We assume the ego agent's goal position is given by some high-level planner and is notated $s_e^g \in \mathbb{R}^{d_s}$.

Let $\mathcal{O}_s \subset \mathcal{O}$ denote the subset of surrounding agents that may interact with the ego agents. Given the information $(S_e^{\text{hist}}, S_{\mathcal{O}}^{\text{hist}}, M, s_e^g)$, for the future $H_2 \in \mathbb{N}$ timesteps, we aim to plan the ego agent's trajectory $S_e^{\text{future}} = (s_e^{t_0+1}, s_e^{t_0+2}, \dots, s_e^{t_0+H_2}) \in \mathbb{R}^{H_2 \times d_s}$, and predict the trajectories of surrounding agents $S_{\mathcal{O}_s}^{\text{future}} = (s_o^{t_0+1}, s_o^{t_0+2}, \dots, s_o^{t_0+H_2})_{o \in \mathcal{O}_s} \in \mathbb{R}^{N_{\mathcal{O}_s} \times (H_2) \times d_s}$, where $N_{\mathcal{O}_s} = |\mathcal{O}_s|$. This joint prediction and planning naturally captures interactive behaviors between agents. Additionally, the planned trajectory for the ego vehicle should satisfy $N_c \in \mathbb{N}$ constraints $c_i(S_e^{\text{future}}) \leq 0, i = 1, 2, \dots, N_c$, which may include goal reaching, control limits, or other requirements.

IV. PRELIMINARIES

A. Motion-Transformer Encoder

To encode the trajectory history $(S_e^{\text{hist}}, S_{\mathcal{O}}^{\text{hist}})$ and map information M as the conditional input for the consistency model, we adopt the encoder architecture from MTR [45, 46]. This transformer-based architecture effectively models scene context through a local attention mechanism, enabling efficient interaction modeling between agents and the road map while maintaining memory efficiency. It also introduces a dense prediction head with a loss function $\mathcal{L}_{\text{encoder}}$ to train this encoder individually. For more detailed descriptions of this encoder,

we refer readers to the original MTR paper [45]. The MTR++ encoder [46] would be suitable for multi-agent settings, but its implementation is not yet available. More importantly, our method is encoder-agnostic, allowing for flexible choice of any suitable scene encoder to integrate with our consistency model-based predictive planner. We represent the encoded feature of the trajectory history and map with MTR encoder as $\text{MTR}(S_e^{\text{hist}}, S_{\mathcal{O}}^{\text{hist}}) \in \mathbb{R}^{(N_{\mathcal{O}}+1) \times D}$ and $\text{MTR}(M) \in \mathbb{R}^{N_m \times D}$, respectively, where D is the embedded feature dimension.

B. Consistency Model

The consistency model can generate high-quality samples from complex distributions with only one or a few sampling steps [52]. It consists of a forward diffusion process and a reverse process. Let \mathcal{D} be our dataset of trajectories. We first normalize all trajectories in \mathcal{D} using the empirical mean and standard deviation computed across the entire dataset. Let \mathcal{X} be the space of such normalized trajectories, and p_{data} be the data distribution over \mathcal{X} . In the forward process, we first draw an initial sample x_1 from p_{data} . We then apply an increasing noise schedule $\sigma_1, \sigma_2, \dots, \sigma_T$ with $\sigma_1 \approx 0$ to progressively corrupt x_1 through T steps. Specifically, at each step i , we draw a noise sample ϵ from $\mathcal{N}(0, I)$ and set the corrupted data x_i as:

$$x_i = x_1 + \sigma_i \cdot \epsilon, \quad i = 1, 2, \dots, T \quad (1)$$

We choose σ_T large enough so that, when x_1 is repeatedly sampled from p_{data} and corrupted via additive Gaussian noise, the empirical distribution of the resulting x_T approximates $\mathcal{N}(0, \sigma_T^2 I)$.

Let \mathcal{Y} be the space of conditioning information. In the reverse process, we aim to learn a consistency function f_{θ} with the parameter θ that maps a noisy trajectory sample x_i , condition $y \in \mathcal{Y}$, and the noise level σ_i directly to the corresponding clean sample x_1 for each step $i = 1, \dots, T$. This is achieved by choosing a specific function form of f_{θ} :

$$f_{\theta}(x, y, \sigma) = c_{\text{skip}}(\sigma)x + c_{\text{out}}(\sigma)F_{\theta}(x, y, \sigma) \quad (2)$$

where σ represents the noise level, and the differentiable function c_{skip} and c_{out} are chosen such that $c_{\text{skip}}(\sigma_1) = 1, c_{\text{out}}(\sigma_1) = 0$ when $\sigma = \sigma_1$ [28]. This ensures that the boundary condition of f_{θ} is met: $f_{\theta}(x_1, y, \sigma_1) = x_1$. F_{θ} is usually approximated by the neural network using a U-Net [40] or a transformer [36] based architecture.

For the consistency model training, we aim to enforce the consistency of the output from f_{θ} for adjacent sampling steps i and $i+1$ to be both x_1 . Let $\mathcal{P}[1, T-1]$ be a distribution over the integer set $1, 2, \dots, T-1$. The consistency training minimizes the following loss function $\mathcal{L}_{\text{consistency}}$:

$$\begin{aligned} \mathcal{L}_{\text{consistency}} = & \mathbb{E}_{i \sim \mathcal{P}[1, T-1], \epsilon \sim \mathcal{N}(0, I)} [d(f_{\theta}(x_i, y, \sigma_i) - f_{\theta}(x_{i+1}, y, \sigma_{i+1}))] \end{aligned} \quad (3)$$

where \mathcal{P} can be the uniform distribution or lognormal distribution, and d is chosen to be a pseudo-huber metric function $d(x, y) = \sqrt{\|x - y\|_2^2 + x^2 - c}$ [50].

During the data generation process, we first draw a sample x_T from $\mathcal{N}(0, \sigma_T^2 I)$. Then with the trained consistency model f_θ , we perform iterative sampling by first predicting the approximate clean data $x_1^{[i]}$ and then sample x_{i-1} with ϵ drawn from $\mathcal{N}(0, I)$:

$$x_1^{[i]} = f_\theta(x_i, y, \sigma_i), \quad x_{i-1} = x_1^{[i]} + \sigma_{i-1}\epsilon \quad (4)$$

for $i = T, T-1, \dots, 1$, until we obtain the final clean sample $x_1^{[1]}$.

V. METHODOLOGY

With the aforementioned notations and stated problem, our proposed method is summarized in Fig. 1. We first use an MTR encoder to encode the agent’s trajectory history and map information. Then we use a consistency model that takes the conditional input of the ego agent’s planning goal and the MTR-encoded features and generates trajectory plans and predictions for the ego and surrounding agents, respectively. Additional planning constraints for the ego agent are achieved through guided sampling of consistency models.

A. Data pre-processing

For training diffusion models or consistency models, we usually need to normalize the input data. If we jointly model ego and surrounding agents’ future trajectories $(S_e^{\text{future}}, S_{\mathcal{O}_s}^{\text{future}})$, using an ego-centric coordinate system introduces large variances in the data, particularly for surrounding agents whose positions vary significantly across scenarios. Thus the training performance is largely degraded. Instead, we apply a coordinate transformation Γ similar to MTR++ [46] that maps each agent’s trajectory into its own local coordinate frame, centered at its position at the current timestep t_0 . This transformation provides us with data $(\Gamma(S_e^{\text{future}}), \Gamma(S_{\mathcal{O}_s}^{\text{future}})) \in \mathbb{R}^{(N_{\mathcal{O}_s}+1) \times H_2 \times d_s}$ that has substantially reduced variance. We then compute the empirical mean and standard deviation of the transformed trajectories across the dataset and standardize them to zero mean and unit variance. To preserve the relative spatial relationships between agents, we collect the reference states consisting of each agent’s position at timestep t_0 as $\text{Ref}(S_e^{\text{future}}, S_{\mathcal{O}_s}^{\text{future}}) \in \mathbb{R}^{(N_{\mathcal{O}_s}+1) \times d_s}$.

B. Consistency Model Training

Let \mathcal{X} denote the space of transformed future trajectories of the ego vehicle $\Gamma(S_e^{\text{future}})$ and surrounding agents $\Gamma(S_{\mathcal{O}_s}^{\text{future}})$ from Sec. V-A. Let \mathcal{Y} denote the space of conditional inputs, containing encoded historical trajectories $\text{MTR}(S_e^{\text{hist}}, S_{\mathcal{O}_s}^{\text{hist}})$, map features $\text{MTR}(M)$ from Sec. IV-A, ego agent’s goal states s_e^g , and the reference coordinates $\text{Ref}(S_e^{\text{future}}, S_{\mathcal{O}_s}^{\text{future}})$ from Sec. V-A.

Given a planning goal and environment context as the condition $y \in \mathcal{Y}$, we leverage the consistency model [52, 50] to sample future trajectories from the conditional probability distribution $p(\cdot|y)$ over \mathcal{X} . Each trajectory sample represents one possible joint future behavior of the ego vehicle and surrounding agents.

For training our predictive planner, we jointly train the MTR encoder and the consistency model together in one step with a hybrid loss function, which is constructed as a weighted sum of the consistency training loss $\mathcal{L}_{\text{consistency}}$ in Eq. (3) and the dense prediction loss $\mathcal{L}_{\text{encoder}}$ of the MTR encoder from Sec. IV-A as follows:

$$\mathcal{L} = \omega_0 \mathcal{L}_{\text{consistency}} + \omega_1 \mathcal{L}_{\text{encoder}} \quad (5)$$

where ω_0 and ω_1 control the weight of these two losses.

C. Guided Sampling

When generating trajectories with the trained consistency model as described in Sec. IV-B, to impose planning constraints on the ego vehicle’s future trajectory, we present a novel guided sampling approach similar to classifier guidance [13]. Importantly, this guidance is applied solely during sampling at test time, without requiring any modification to the training procedure.

Assuming there are $N_c \in \mathbb{N}$ planning constraint c_j to minimize, $j = 1, 2, \dots, N_c$ and drawing inspiration from classifier guidance [13], we can perform a gradient descent step on the predicted $x_1^{[i]}$ during each sampling step i in Eq. (4):

$$x_1^{[i,1]} = x_1^{[i]} - \sum_{j=1}^{N_c} \alpha_j \nabla c_j \quad (6)$$

where ∇c_j represents the first-order gradient of the planning constraint c_j and can be computed using auto-differentiation. α_j is the corresponding step size for each constraint c_j . Then the tuned $x_1^{[i,1]}$ is used to sample x_{i-1} in Eq. (4).

However, optimizing multiple constraints simultaneously presents a significant challenge in finding a suitable stepsize α efficiently, particularly when constraints may conflict with each other. To address this challenge, inspired by the Alternating Direction Method of Multipliers (ADMM) [6], we propose a novel alternating direction method that only optimizes one constraint at a time during each sampling step i :

$$\begin{aligned} x_1^{[i,1]} &= x_1^{[i]} - \alpha_1 \nabla c_1 \\ x_1^{[i,2]} &= x_1^{[i,1]} - \alpha_2 \nabla c_2 \\ &\dots \\ x_1^{[i,N_c]} &= x_1^{[i,N_c-1]} - \alpha_{N_c} \nabla c_{N_c} \end{aligned} \quad (7)$$

In our approach, we sequentially optimize each constraint c_j with corresponding step sizes α_j during each gradient descent iteration. While our selection of the optimization order and relatively small step sizes is based on empirical observations, this strategy has demonstrated effective convergence in practice, which is difficult to achieve with the standard guidance method with gradient descent in Eq. (6). The convergence of alternating direction methods, such as ADMM, is generally guaranteed under conditions including closed, proper, and convex functions and appropriately chosen step sizes [6].

D. Planning Constraints Construction

We assume that the ego vehicle’s dynamics are as follows:

$$\dot{p}_x = v \cos \theta, \quad \dot{p}_y = v \sin \theta, \quad \dot{v} = a, \quad \dot{\theta} = \omega \quad (8)$$

where p_x and p_y are positions, v is the linear speed and θ is the orientation. The control input is the acceleration a and angular speed ω .

Suppose we only use p_x and p_y from ego agent’s future states S_e^{future} to construct our planning constraint function c_i , since other states like v or θ may not satisfy the dynamics equations in Eq. (8) and are also quite noisy. Using the property of differential flatness for dynamics in Eq. (8), we can infer v and θ with p_x and p_y as follows:

$$v = \sqrt{\dot{p}_x^2 + \dot{p}_y^2}, \quad \theta = \arctan\left(\frac{\dot{p}_y}{\dot{p}_x}\right) \quad (9)$$

Then we can further infer the control input a and ω :

$$a = \frac{\dot{p}_x \ddot{p}_x + \dot{p}_y \ddot{p}_y}{\sqrt{\dot{p}_x^2 + \dot{p}_y^2}}, \quad \omega = \frac{\dot{p}_x \ddot{p}_y - \dot{p}_y \ddot{p}_x}{\dot{p}_x^2 + \dot{p}_y^2} \quad (10)$$

Note that, a and v are computed through finite differencing of p_x and p_y which will inevitably incur some noises.

With p_x, p_y and the derived a and ω , we consider three types of planning constraint c to minimize as follows.

$$\begin{aligned} c_{\text{goal}} &= \sqrt{(p_x^{t_0+H_2} - p_{x,\text{goal}})^2 + (p_y^{t_0+H_2} - p_{y,\text{goal}})^2} \\ c_{\text{acc}} &= \frac{1}{H_2} \sum_{i=t_0}^{t_0+H_2} \max(|a^i| - a_{\text{limit}}, 0) \\ c_{\omega} &= \frac{1}{H_2} \sum_{i=t_0}^{t_0+H_2} \max(|\omega^i| - \omega_{\text{limit}}, 0) \end{aligned} \quad (11)$$

c_{goal} represents a goal-reaching constraint such that the ego vehicle needs to reach a pre-specified goal $(p_{x,\text{goal}}, p_{y,\text{goal}})$ at the final timestep $t_0 + H_2$. c_{acc} and c_{ω} are control limit constraints that compute the average control limit violation along the ego agent’s trajectory for a given a_{limit} and ω_{limit} .

VI. EXPERIMENTS

A. Experiment setup

1) **Dataset:** We evaluate our method on the Waymo Open Motion Dataset (WOMD) [15], which contains 486k traffic scenarios in the training set and 44k scenarios in the validation set that we can test on. Each scenario provides road graph information and trajectories of diverse agents including vehicles, pedestrians, and cyclists, with up to 8 agents specifically marked for trajectory prediction. For each agent, this dataset includes 1 second of history, current state, and 8 seconds of future trajectory, sampled at 0.1-second intervals. This sets our history horizon to be $H_1 = 10$ and future horizons to be $H_2 = 80$ timesteps, respectively. For each scenario, with the trajectory information from all agents including vehicles, pedestrians, and cyclists as $S_{\mathcal{O}}$, we only select vehicle agents as the ego agent with trajectories denoted by S_e . We then identify the surrounding agents, with trajectories denoted as

TABLE I: Planning Trajectory Compared to the Human Groundtruth

Method	minADE ↓	minFDE ↓
Transformer	0.944	3.239
DDPM-10	0.346	0.377
DDPM-4	0.363	0.498
DDIM-4	2.126	2.559
Consistency	0.309	0.218
Consistency (guided)	0.303	0.016

$S_{\mathcal{O}_s}$, by selecting up to 4 agents closest to the ego vehicle based on their trajectory distances, excluding those beyond a 10-meter threshold. This enables us to focus our predictive planner on the most relevant interactive behaviors between the ego vehicle and its immediate surroundings. The goal s_e^g of the ego agent is chosen as its state at the end of the 8-second future horizon.

2) **Model Details:** The MTR encoder consists of 6 transformer layers with a dimension of 256 to encode agent trajectory histories and map information into $\text{MTR}(S_e^{\text{hist}}, S_{\mathcal{O}}^{\text{hist}}, M)$. For detailed encoder architecture specifications, we refer readers to [45]. The conditional input y for the consistency model is constructed by further encoding three components: the obtained features $\text{MTR}(S_e^{\text{hist}}, S_{\mathcal{O}}^{\text{hist}}, M)$, the ego agent’s goal s_e^g , and the reference states $\text{Ref}(S_e^{\text{future}}, S_{\mathcal{O}_s}^{\text{future}})$, using 3-layer MLPs with 256 neurons per layer. To model the consistency model function F_{θ} , we adopt the U-Net [40] with the model dimension of 128 as the backbone.

For the consistency model, we choose $T = 5$ which indicates 4 sampling steps in the forward and reverse process. Follow the original paper [50], we set the noise schedule with $\rho = 6$, $\sigma_1 = 0.002$, $\sigma_T = 80$, and then $\sigma_i = \left(\sigma_0^{1/\rho} + \frac{i-1}{T-1}(\sigma_T^{1/\rho} - \sigma_0^{1/\rho})\right)^\rho$, $i = 1, \dots, T$. During guided sampling, we perform 100 gradient steps of Eq. (7) at each sampling step, and set the coefficient for c_{goal} , c_{acc} and c_{ω} to be 2×10^{-5} , 3×10^{-6} , 5×10^{-7} , respectively.

3) **Methods and Baselines:** We compare our consistency model-based approach against several baselines. Currently, we only provide the evaluation of the open-loop trajectory generation performance of those methods, focusing on the behavior through a single inference step.

a) **Transformer:** A model based on MTR’s encoder-decoder architecture [45] to generate trajectory only for ego vehicle. It has a larger model size for the decoder (512 vs. our 128), but doesn’t incorporate ego vehicle’s goal s_e^g as input.

b) **DDPM:** This diffusion baseline uses the same MTR encoder and MLP architecture as ours for condition encoding but adopts DDPM [20] for trajectory sampling of ego and surrounding agents. Note that it differs from consistency models in both its forward diffusion process and training loss function. We evaluate two variants: one trained and sampled with 4 steps (DDPM-4), and another trained and sampled with 10 steps (DDPM-10).

c) **DDIM:** This baseline extends DDPM-10 by incorporating the more efficient DDIM sampling strategy [48]. While

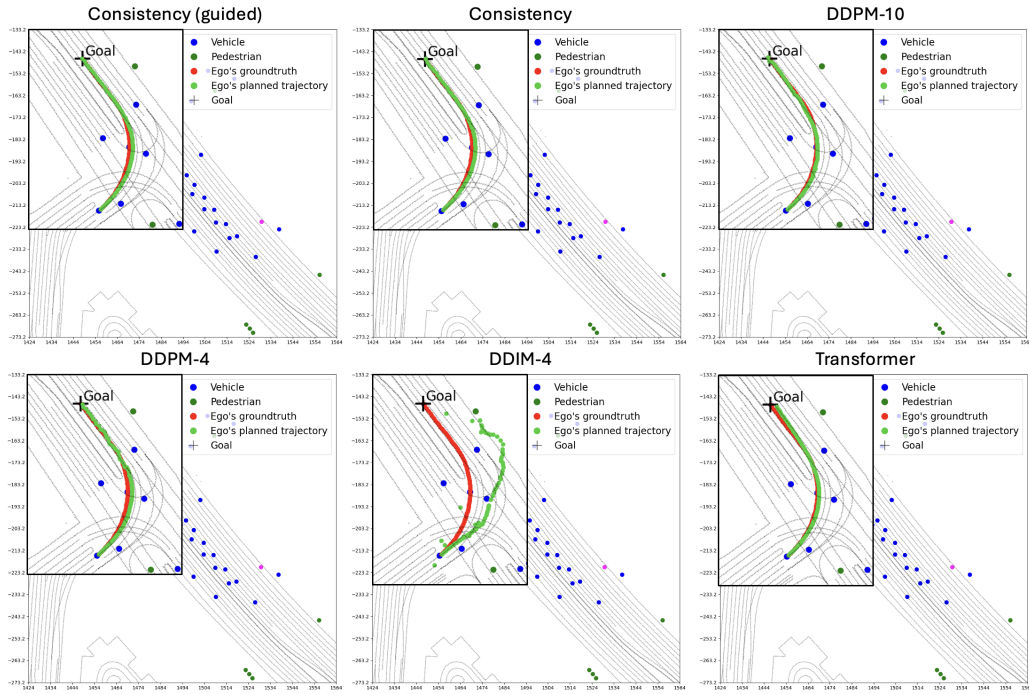


Fig. 2: Ego vehicle’s planned trajectory (Green) in a left-turn scenario compared to the Groundtruth (Red).

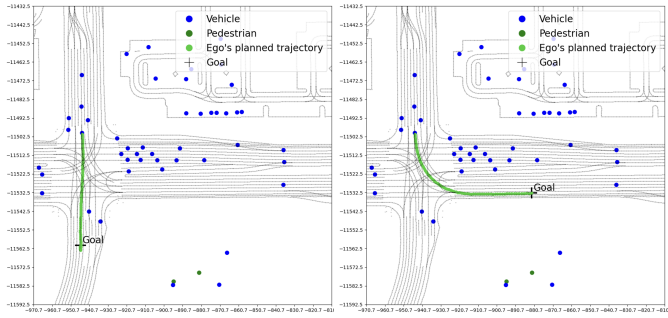


Fig. 3: Planning with different goal locations using consistency models and guided sampling.

using the same training process as DDPM-10, it employs 4-step DDIM sampling during inference, denoted as DDIM-4.

d) Consistency: Our proposed consistency model is trained and sampled with 4 steps.

e) Consistency (guided): Our proposed consistency model is trained and sampled with 4 steps, with guided sampling.

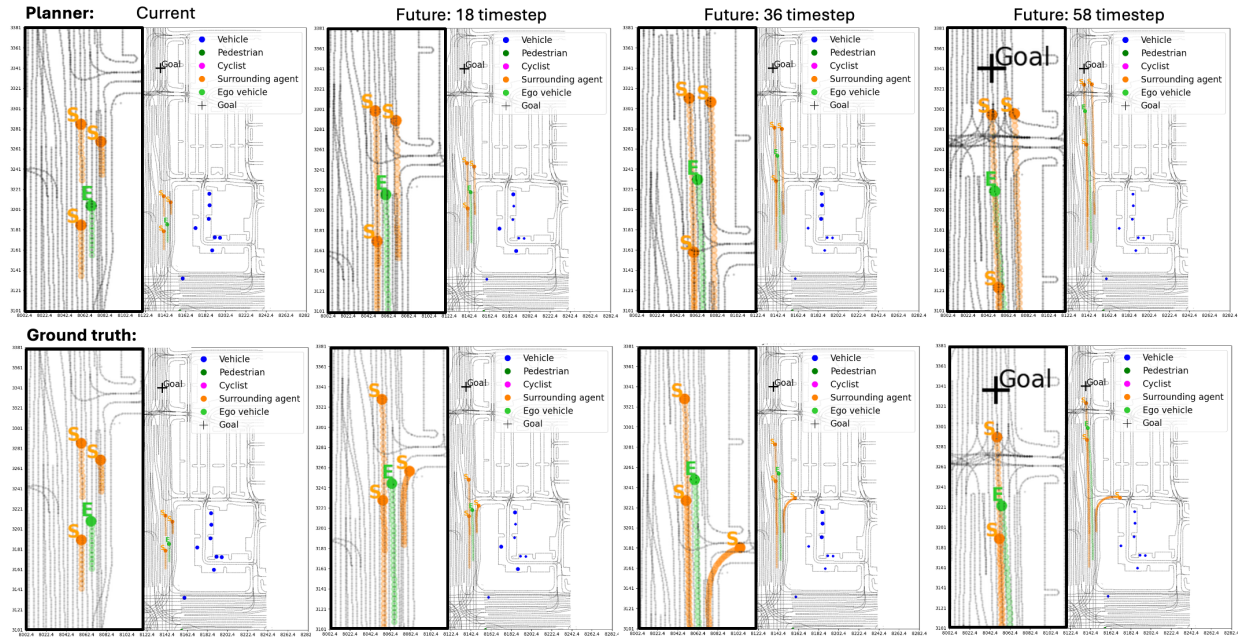
4) Training: We conduct distributed training with a total batch size of 100 across 4 NVIDIA L40 GPUs, each with a batch size of 25. For consistency and diffusion models, we use the Adam optimizer [29] with a learning rate of 8×10^{-5} and train for 50 epochs. For the transformer, we follow the MTR settings [45] and use the AdamW optimizer [35] with a learning rate of 1×10^{-4} and weight decay of 0.01, and train for 30 epochs.

B. Experiment results and analysis

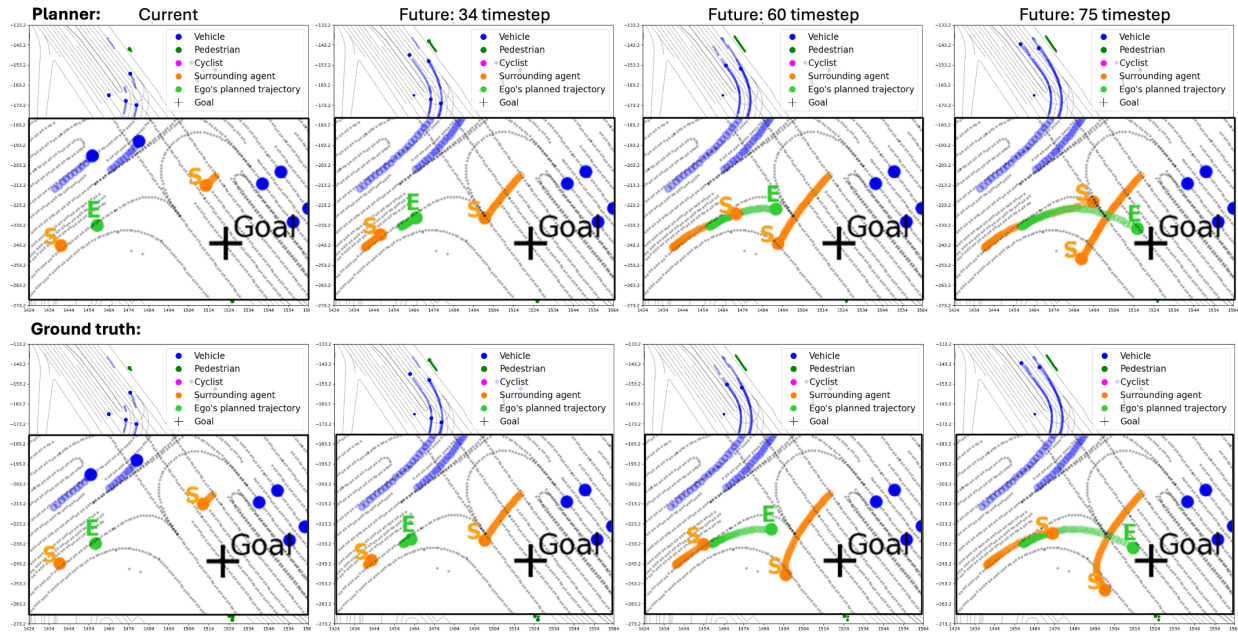
In this section, we evaluate our consistency model-based planner from several aspects. First, we assess its planning performance and trajectory quality compared to several baseline methods. Then we take a closer look at interactive scenarios and present examples of proactive nudging and yielding behaviors of our predictive planner. Furthermore, we show how online guided sampling improves constraint satisfaction in planning - the controllability not provided with transformer-based approaches. Finally, we discuss the computational time during inference for our presented methods.

1) Trajectory Planning Performance: In Fig. 2, we compare planned trajectories generated by different methods (shown in green) against the ground truth from the dataset (shown in red). The scenario requires the ego vehicle to make a left turn and then drive straight to reach its goal. According to Fig. 2, DDPM-4 reaches the goal but produces a noisy trajectory, likely due to insufficient sampling steps for diffusion models to generate high-quality trajectories. While DDPM-10’s increased sampling steps yields slightly smoother trajectories, it comes at the cost of longer computation time. DDIM-4 attempts to accelerate DDPM-10 using only 4 sampling steps, but fails to generate goal-reaching trajectories. The transformer with a larger model size generates a trajectory close to the ground truth but misses the exact goal location. In contrast, our consistency model generates smooth trajectories that both align with the ground truth and precisely reach the target location.

In Table I, we quantitatively evaluate the planning performance for the ego vehicle compared to the human groundtruth through metrics from Waymo’s Motion Prediction Challenge



(a) A proactive nudging behavior from the ego car to switch a lane.



(b) A yielding behavior for the ego car to make a turn.

Fig. 4: For each scenario, upper row: interactive behavior from our predictive planner; lower row: Ground truth driving behaviors. The ego agent’s trajectory is in green annotated by “E” and the surrounding agents’ trajectories are in orange annotated by “S”. The other agents’ trajectories (always shown with ground truth) are in blue.

[58]: Minimum Average Displacement Error (minADE) and Minimum Final Displacement Error (minFDE) on the entire test dataset. Here we view these metrics as an evaluation of how closely our generated trajectories align with human driving behavior under the same environmental context and goal conditions. The results align with our qualitative observations: our consistency model achieves the lowest minADE and minFDE, indicating that it captures human driving patterns

well. Moreover, the addition of guided sampling significantly improves the minFDE for the consistency models since it explicitly incorporates goal-reaching constraints.

In Table II, we evaluate the trajectory quality using three metrics that characterize driving behavior: 1) angle changes, which measure the smoothness of directional transitions, 2) path length, which quantifies the efficiency of the chosen route, and 3) curvature, which assesses the sharpness of turns. Lower

TABLE II: Planning Trajectory Quality

Method	Angle changes ↓	Path len ↓	Curvature ↓
Transformer	0.419	59.621	0.560
DDPM-10	0.660	87.801	3.444
DDPM-4	0.729	79.731	2.211
DDIM-4	0.683	157.78	2.012
Consistency	0.636	58.060	1.174
Consistency (guided)	0.445	57.564	0.610

values in these metrics generally indicate smoother and more efficient trajectories that align with natural driving patterns. Our consistency model achieves superior trajectory quality compared to all diffusion-based methods, including DDPM-10 despite its additional sampling steps. While the transformer method has slightly lower angle changes and curvature, this is expected given its substantially larger model size (512 vs. our 128 dimensions).

Furthermore, we demonstrate the flexibility of our approach in choosing goal location in Fig. 3. Our consistency model maintains high-quality trajectory planning when targeting novel goal locations, even when they are not present in the dataset. The current transformer method with MTR doesn’t support the selection of goal locations.

2) *Interactive Behavior*: A key advantage of our predictive planner is its ability to ensure safe and effective interactions with other road users in traffic. Our planner demonstrates the capability for generating both proactive behaviors as shown in Fig. 4, such as nudging for lane switching and yielding to pedestrians. The ego agent (labeled “E”) trajectory is in green and the surrounding agents (labeled “S”) trajectories are in orange. Other agent’s trajectories are shown in blue. These learned behaviors are similar to ground truth human drivers and ensure efficient navigation and safe interaction between the ego vehicle and other road users. Crucially, all planning and prediction are achieved through a single inference of the consistency model.

In Fig. 4a, we show a proactive nudging scenario. Here, the ego vehicle needs to merge into the left lane while a nearby vehicle occupies that lane. Our planner directs the ego vehicle to accelerate and nudge into the left lane, predicting that the vehicle in the left lane will decelerate to accommodate the lane change. This nudging behavior demonstrates the proactive planning capability of our end-to-end, data-driven predictive planner, which is challenging to achieve using modular methods. While in the ground truth, the left car doesn’t decelerate that much and the rightmost vehicle eventually turns right, this discrepancy is expected given that we currently generate 8-second future trajectories through a single inference.

In Fig. 4b, a yielding behavior is presented. The ego vehicle intends to make a right turn but predicts that a pedestrian will continue crossing the road. As a result, the planner instructs the ego vehicle to wait until the pedestrian has fully crossed, which is highly aligned with the ground truth. This yielding behavior ensures safe interaction between the ego vehicle and other road users, highlighting the planner’s safe operation in

TABLE III: Planning Constraint Violations

Method	Goal Reaching ↓	Acc limit ↓	ω limit ↓
Transformer	9.256	0.570	1.029
DDPM-10	12.669	80.581	3.307
DDPM-4	13.873	56.170	3.323
DDIM-4	22.933	218.823	5.270
Consistency	0.618	5.754	2.050
Consistency (guided)	0.127	0.462	0.599

TABLE IV: Computational Time Comparison for Inference

Method	Inference Time (s)
Transformer	1.910
DDPM-10	3.352
DDPM-4	2.226
DDIM-4	2.118
Consistency	2.301
Consistency (Guided)	2.635

dynamic environments.

3) *Guided Sampling*: The guided sampling approach described in Sec. V-C and Sec. V-D allows us to enforce planning constraints during inference time, providing a key advantage over transformer-based methods which lack this capability. We quantitatively evaluate all methods against three planning constraints from Eq. (11): goal reaching, acceleration limits, and orientation speed limits. As shown in Table III, our base consistency model already achieves more accurate goal-reaching and smoother behaviors than other diffusion-based approaches. With guided sampling, these planning constraint violations of the consistency model further decrease by a factor of 4, achieving the lowest values among all methods. Note that this improvement requires no model retraining and only applies during inference.

4) *Computational time discussions*: All methods in our evaluation support batch sampling. As shown in Table IV, we evaluate their inference times using a batch of 30 scenarios with 125 ego agents on an NVIDIA GeForce RTX 3060. While the transformer achieves the fastest inference time, it lacks our method’s key capabilities: online controllable generation and sampling from multimodal joint distribution. Our consistency model achieves a similar inference time with DDPM-4 and DDIM-4 due to the same model dimensionality, and sampling steps. However, DDPM-4 and DDIM-4 fail to match our consistency model’s performance in trajectory generation across all metrics, as evidenced in Fig. 2, Table I, Table II, and Table III. The guided sampling, introducing a little computational overhead, provides higher quality trajectory generation and enables controllable planning. Even DDPM-10, despite its increased sampling steps and higher computational time, cannot achieve a comparable performance of trajectory generation to our approach.

VII. LIMITATIONS

Although our proposed method significantly improves the efficiency of generating human-like trajectories through con-

sistency models and joint prediction and planning, it may not yet meet the demands of real-time operation, especially in highly dynamic environments that require high-frequency planning. Future work could leverage model pruning or distillation techniques to further improve the inference efficiency. Besides, while in the current paper, we test open-loop trajectory generation to focus on evaluating the model performance of a single inference step, in the future we will extend our method to the closed-loop case with a receding horizon fashion, which is expected to further enhance the interactive planning.

VIII. CONCLUSIONS

In this paper, we present a novel data-driven approach that unifies trajectory prediction and planning using consistency models. By modeling the joint distribution of ego and surrounding agents' trajectories, our method enables efficient and interactive planning, such as proactive nudging and yielding, without the need for iterative alternation between prediction and planning modules. Trained on the Waymo Open Motion Dataset, the proposed consistency model generates human-like trajectories while its guided sampling capability naturally incorporates additional planning constraints during online trajectory generations. Experimental results demonstrate that our approach achieves superior trajectory quality and interactive behavior compared to existing methods while requiring fewer sampling steps. This framework also has the potential to be extended to broader robot decision-making tasks in interactive scenarios.

Looking forward, we aim to optimize this method for real-time operation and extend it to closed-loop operation with receding horizon planning. Additionally, we plan to incorporate LLMs as high-level planners to interpret diverse contextual information and enhance decision-making in challenging scenarios.

REFERENCES

- [1] Anurag Ajay, Yilun Du, Abhi Gupta, Joshua Tenenbaum, Tommi Jaakkola, and Pulkit Agrawal. Is conditional generative modeling all you need for decision-making? *arXiv preprint arXiv:2211.15657*, 2022.
- [2] Alexandre Miranda Anon, Sangjae Bae, Manish Saroya, and David Isele. Multi-profile quadratic programming (mpqp) for optimal gap selection and speed planning of autonomous driving. *arXiv preprint arXiv:2401.06305*, 2024.
- [3] Sangjae Bae, Dhruv Saxena, Alireza Nakhaei, Chiho Choi, Kikuo Fujimura, and Scott Moura. Cooperation-aware lane change maneuver in dense traffic based on model predictive control with recurrent neural network. In *2020 American Control Conference (ACC)*, pages 1209–1216. IEEE, 2020.
- [4] Sangjae Bae, David Isele, Alireza Nakhaei, Peng Xu, Alexandre Miranda Anon, Chiho Choi, Kikuo Fujimura, and Scott Moura. Lane-change in dense traffic with model predictive control and neural networks. *IEEE*

- Transactions on Control Systems Technology*, 31(2):646–659, 2022.
- [5] Francesca Baldini, Faizan M Tariq, Sangjae Bae, and David Isele. Don't get stuck: A deadlock recovery approach. In *2024 IEEE 27th International Conference on Intelligent Transportation Systems (ITSC)*. IEEE, 2024.
- [6] Stephen Boyd, Neal Parikh, Eric Chu, Borja Peleato, Jonathan Eckstein, et al. Distributed optimization and statistical learning via the alternating direction method of multipliers. *Foundations and Trends® in Machine learning*, 3(1):1–122, 2011.
- [7] Holger Caesar, Varun Bankiti, Alex H Lang, Sourabh Vora, Venice Erin Liong, Qiang Xu, Anush Krishnan, Yu Pan, Giancarlo Baldan, and Oscar Beijbom. nuscenes: A multimodal dataset for autonomous driving. In *Proceedings of the IEEE/CVF conference on computer vision and pattern recognition*, pages 11621–11631, 2020.
- [8] Ming-Fang Chang, John Lambert, Patsorn Sangkloy, Jagjeet Singh, Slawomir Bak, Andrew Hartnett, De Wang, Peter Carr, Simon Lucey, Deva Ramanan, et al. Argoverse: 3d tracking and forecasting with rich maps. In *Proceedings of the IEEE/CVF conference on computer vision and pattern recognition*, pages 8748–8757, 2019.
- [9] Wei-Jer Chang, Francesco Pittaluga, Masayoshi Tomizuka, Wei Zhan, and Manmohan Chandraker. Controllable safety-critical closed-loop traffic simulation via guided diffusion. *arXiv preprint arXiv:2401.00391*, 2023.
- [10] Yuxiao Chen, Sushant Veer, Peter Karkus, and Marco Pavone. Interactive joint planning for autonomous vehicles. *IEEE Robotics and Automation Letters*, 2023.
- [11] Cheng Chi, Siyuan Feng, Yilun Du, Zhenjia Xu, Eric Cousineau, Benjamin Burchfiel, and Shuran Song. Diffusion policy: Visuomotor policy learning via action diffusion. *arXiv preprint arXiv:2303.04137*, 2023.
- [12] Sandra Devin and Rachid Alami. An implemented theory of mind to improve human-robot shared plans execution. In *2016 11th ACM/IEEE International Conference on Human-Robot Interaction (HRI)*, pages 319–326. IEEE, 2016.
- [13] Prafulla Dhariwal and Alexander Nichol. Diffusion models beat gans on image synthesis. *Advances in neural information processing systems*, 34:8780–8794, 2021.
- [14] Zihan Ding and Chi Jin. Consistency models as a rich and efficient policy class for reinforcement learning. *arXiv preprint arXiv:2309.16984*, 2023.
- [15] Scott Ettinger, Shuyang Cheng, Benjamin Caine, Chenxi Liu, Hang Zhao, Sabeek Pradhan, Yuning Chai, Ben Sapp, Charles R Qi, Yin Zhou, et al. Large scale interactive motion forecasting for autonomous driving: The waymo open motion dataset. In *Proceedings of the IEEE/CVF International Conference on Computer Vision*, pages 9710–9719, 2021.
- [16] Jaime F Fisac, Eli Bronstein, Elis Steffansson, Dorsa Sadigh, S Shankar Sastry, and Anca D Dragan. Hierarchical game-theoretic planning for autonomous vehi-

- cles. In *2019 International conference on robotics and automation (ICRA)*, pages 9590–9596. IEEE, 2019.
- [17] Piyush Gupta, David Isele, Donggun Lee, and Sangjae Bae. Interaction-aware trajectory planning for autonomous vehicles with analytic integration of neural networks into model predictive control. In *2023 IEEE International Conference on Robotics and Automation (ICRA)*, pages 7794–7800. IEEE, 2023.
- [18] Piyush Gupta, David Isele, and Sangjae Bae. Towards scalable & efficient interaction-aware planning in autonomous vehicles using knowledge distillation. *arXiv preprint arXiv:2404.01746*, 2024.
- [19] Jonathan Ho and Tim Salimans. Classifier-free diffusion guidance. *arXiv preprint arXiv:2207.12598*, 2022.
- [20] Jonathan Ho, Ajay Jain, and Pieter Abbeel. Denoising diffusion probabilistic models. *Advances in neural information processing systems*, 33:6840–6851, 2020.
- [21] Jonathan Ho, Tim Salimans, Alexey Gritsenko, William Chan, Mohammad Norouzi, and David J Fleet. Video diffusion models. *Advances in Neural Information Processing Systems*, 35:8633–8646, 2022.
- [22] Haimin Hu, David Isele, Sangjae Bae, and Jaime F Fisac. Active uncertainty reduction for safe and efficient interaction planning: A shielding-aware dual control approach. *The International Journal of Robotics Research*, 43(9):1382–1408, 2024.
- [23] Yeping Hu, Wei Zhan, and Masayoshi Tomizuka. Scenario-transferable semantic graph reasoning for interaction-aware probabilistic prediction. *IEEE Transactions on Intelligent Transportation Systems*, 23(12):23212–23230, 2022.
- [24] Zhiyu Huang, Zixu Zhang, Ameeya Vaidya, Yuxiao Chen, Chen Lv, and Jaime Fernández Fisac. Versatile scene-consistent traffic scenario generation as optimization with diffusion. *arXiv preprint arXiv:2404.02524*, 2024.
- [25] David Isele. Interactive decision making for autonomous vehicles in dense traffic. In *2019 IEEE Intelligent Transportation Systems Conference (ITSC)*, pages 3981–3986. IEEE, 2019.
- [26] Michael Janner, Yilun Du, Joshua B Tenenbaum, and Sergey Levine. Planning with diffusion for flexible behavior synthesis. *arXiv preprint arXiv:2205.09991*, 2022.
- [27] Chiyu Jiang, Andre Cornman, Cheolho Park, Benjamin Sapp, Yin Zhou, Dragomir Anguelov, et al. Motiondiffuser: Controllable multi-agent motion prediction using diffusion. In *Proceedings of the IEEE/CVF Conference on Computer Vision and Pattern Recognition*, pages 9644–9653, 2023.
- [28] Tero Karras, Miika Aittala, Timo Aila, and Samuli Laine. Elucidating the design space of diffusion-based generative models. *Advances in neural information processing systems*, 35:26565–26577, 2022.
- [29] Diederik P Kingma. Adam: A method for stochastic optimization. *arXiv preprint arXiv:1412.6980*, 2014.
- [30] Sergey Levine, Chelsea Finn, Trevor Darrell, and Pieter Abbeel. End-to-end training of deep visuomotor policies. *Journal of Machine Learning Research*, 17(39):1–40, 2016.
- [31] Anjian Li, Liting Sun, Wei Zhan, Masayoshi Tomizuka, and Mo Chen. Prediction-based reachability for collision avoidance in autonomous driving. In *2021 IEEE International Conference on Robotics and Automation (ICRA)*, pages 7908–7914. IEEE, 2021.
- [32] Anjian Li, Zihan Ding, Adji Bousso Dieng, and Ryne Beeson. Constraint-aware diffusion models for trajectory optimization. *arXiv preprint arXiv:2406.00990*, 2024.
- [33] Anjian Li, Zihan Ding, Adji Bousso Dieng, and Ryne Beeson. Efficient and guaranteed-safe non-convex trajectory optimization with constrained diffusion model. *arXiv preprint arXiv:2403.05571*, 2024.
- [34] Jinning Li, Jiachen Li, Sangjae Bae, and David Isele. Adaptive prediction ensemble: Improving out-of-distribution generalization of motion forecasting. *IEEE Robotics and Automation Letters*, 2024.
- [35] I Loshchilov. Decoupled weight decay regularization. *arXiv preprint arXiv:1711.05101*, 2017.
- [36] William Peebles and Saining Xie. Scalable diffusion models with transformers. In *Proceedings of the IEEE/CVF International Conference on Computer Vision*, pages 4195–4205, 2023.
- [37] Aaditya Prasad, Kevin Lin, Jimmy Wu, Linqi Zhou, and Jeannette Bohg. Consistency policy: Accelerated visuomotor policies via consistency distillation. *arXiv preprint arXiv:2405.07503*, 2024.
- [38] Davis Rempe, Zhengyi Luo, Xue Bin Peng, Ye Yuan, Kris Kitani, Karsten Kreis, Sanja Fidler, and Or Litany. Trace and pace: Controllable pedestrian animation via guided trajectory diffusion. In *Proceedings of the IEEE/CVF Conference on Computer Vision and Pattern Recognition*, pages 13756–13766, 2023.
- [39] Robin Rombach, Andreas Blattmann, Dominik Lorenz, Patrick Esser, and Björn Ommer. High-resolution image synthesis with latent diffusion models. In *Proceedings of the IEEE/CVF conference on computer vision and pattern recognition*, pages 10684–10695, 2022.
- [40] Olaf Ronneberger, Philipp Fischer, and Thomas Brox. U-net: Convolutional networks for biomedical image segmentation. In *Medical image computing and computer-assisted intervention—MICCAI 2015: 18th international conference, Munich, Germany, October 5-9, 2015, proceedings, part III 18*, pages 234–241. Springer, 2015.
- [41] Dorsa Sadigh, Shankar Sastry, Sanjit A Seshia, and Anca D Dragan. Planning for autonomous cars that leverage effects on human actions. In *Robotics: Science and systems*, volume 2, pages 1–9. Ann Arbor, MI, USA, 2016.
- [42] Tim Salimans and Jonathan Ho. Progressive distillation for fast sampling of diffusion models. *arXiv preprint arXiv:2202.00512*, 2022.
- [43] Tim Salzmann, Boris Ivanovic, Punarjay Chakravarty, and Marco Pavone. Trajectron++: Dynamically-feasible

- trajectory forecasting with heterogeneous data. In *Computer Vision—ECCV 2020: 16th European Conference, Glasgow, UK, August 23–28, 2020, Proceedings, Part XVIII 16*, pages 683–700. Springer, 2020.
- [44] Dhruv Mauria Saxena, Sangjae Bae, Alireza Nakhaei, Kikuo Fujimura, and Maxim Likhachev. Driving in dense traffic with model-free reinforcement learning. In *2020 IEEE International Conference on Robotics and Automation (ICRA)*, pages 5385–5392. IEEE, 2020.
- [45] Shaoshuai Shi, Li Jiang, Dengxin Dai, and Bernt Schiele. Motion transformer with global intention localization and local movement refinement. *Advances in Neural Information Processing Systems*, 35:6531–6543, 2022.
- [46] Shaoshuai Shi, Li Jiang, Dengxin Dai, and Bernt Schiele. Mtr++: Multi-agent motion prediction with symmetric scene modeling and guided intention querying. *IEEE Transactions on Pattern Analysis and Machine Intelligence*, 2024.
- [47] Jascha Sohl-Dickstein, Eric Weiss, Niru Maheswaranathan, and Surya Ganguli. Deep unsupervised learning using nonequilibrium thermodynamics. In *International conference on machine learning*, pages 2256–2265. PMLR, 2015.
- [48] Jiaming Song, Chenlin Meng, and Stefano Ermon. Denoising diffusion implicit models. *arXiv preprint arXiv:2010.02502*, 2020.
- [49] Lin Song, David Isele, Naira Hovakimyan, and Sangjae Bae. Efficient and interaction-aware trajectory planning for autonomous vehicles with particle swarm optimization. *arXiv preprint arXiv:2402.01575*, 2024.
- [50] Yang Song and Prafulla Dhariwal. Improved techniques for training consistency models. *arXiv preprint arXiv:2310.14189*, 2023.
- [51] Yang Song, Jascha Sohl-Dickstein, Diederik P Kingma, Abhishek Kumar, Stefano Ermon, and Ben Poole. Score-based generative modeling through stochastic differential equations. *arXiv preprint arXiv:2011.13456*, 2020.
- [52] Yang Song, Prafulla Dhariwal, Mark Chen, and Ilya Sutskever. Consistency models. *arXiv preprint arXiv:2303.01469*, 2023.
- [53] Andrea Thomaz, Guy Hoffman, Maya Cakmak, et al. Computational human-robot interaction. *Foundations and Trends® in Robotics*, 4(2-3):105–223, 2016.
- [54] Ran Tian, Liting Sun, Masayoshi Tomizuka, and David Isele. Anytime game-theoretic planning with active reasoning about humans’ latent states for human-centered robots. In *2021 IEEE International Conference on Robotics and Automation (ICRA)*, pages 4509–4515. IEEE, 2021.
- [55] Ran Tian, Liting Sun, Andrea Bajcsy, Masayoshi Tomizuka, and Anca D Dragan. Safety assurances for human-robot interaction via confidence-aware game-theoretic human models. In *2022 International Conference on Robotics and Automation (ICRA)*, pages 11229–11235. IEEE, 2022.
- [56] A Vaswani. Attention is all you need. *Advances in Neural Information Processing Systems*, 2017.
- [57] Yixiao Wang, Chen Tang, Lingfeng Sun, Simone Rossi, Yichen Xie, Chensheng Peng, Thomas Hannagan, Stefano Sabatini, Nicola Poerio, Masayoshi Tomizuka, et al. Optimizing diffusion models for joint trajectory prediction and controllable generation. In *European Conference on Computer Vision*, pages 324–341. Springer, 2025.
- [58] Waymo. Motion prediction – 2024 – Waymo open dataset. <https://waymo.com/open/challenges/2024/motion-prediction/>, 2024. Accessed: December 19, 2024.
- [59] Chejian Xu, Ding Zhao, Alberto Sangiovanni-Vincentelli, and Bo Li. Diffscene: Diffusion-based safety-critical scenario generation for autonomous vehicles. In *The Second Workshop on New Frontiers in Adversarial Machine Learning*, 2023.
- [60] Wenda Xu, Junqing Wei, John M Dolan, Huijing Zhao, and Hongbin Zha. A real-time motion planner with trajectory optimization for autonomous vehicles. In *2012 IEEE International Conference on Robotics and Automation*, pages 2061–2067. IEEE, 2012.
- [61] Wenda Xu, Qian Wang, and John M Dolan. Autonomous vehicle motion planning via recurrent spline optimization. In *2021 IEEE International Conference on Robotics and Automation (ICRA)*, pages 7730–7736. IEEE, 2021.
- [62] Wei Zhan, Liting Sun, Di Wang, Haojie Shi, Aubrey Clausse, Maximilian Naumann, Julius Kummerle, Hendrik Konigshof, Christoph Stiller, Arnaud de La Fortelle, et al. Interaction dataset: An international, adversarial and cooperative motion dataset in interactive driving scenarios with semantic maps. *arXiv preprint arXiv:1910.03088*, 2019.
- [63] Ziyuan Zhong, Davis Rempe, Danfei Xu, Yuxiao Chen, Sushant Veer, Tong Che, Baishakhi Ray, and Marco Pavone. Guided conditional diffusion for controllable traffic simulation. In *2023 IEEE International Conference on Robotics and Automation (ICRA)*, pages 3560–3566. IEEE, 2023.